

IMECE2010-39153

ANALYTICAL METHOD TO DETERMINE THE TERTIARY CREEP DAMAGE CONSTANTS OF THE KACHANOV-RABOTNOV CONSTITUTIVE MODEL

Calvin M. Stewart

Department of Mechanical, Materials, & Aerospace
Engineering, University of Central Florida
Orlando, FL USA 32816-2450

Ali P. Gordon

Department of Mechanical, Materials, & Aerospace
Engineering, University of Central Florida
Orlando, FL USA 32816-2450

ABSTRACT

The classic Kachanov-Rabotnov isotropic creep damage constitutive model has been used in many situations to predict the creep deformation of high temperature components. Typically, the secondary creep behavior is determined by analytical methods; however, the tertiary creep damage constants are found using a mixture of trial and error and numerical optimization. These methods require substantial hand calculations and computational time to determine the tertiary creep damage constants. In this paper, a novel analytical method is developed to determine the tertiary creep damage constants. Comparisons between numerical optimized constants and those found using the analytical method are given for a Ni-based superalloy. Creep deformation, damage evolution, and rupture time predictions are compared. A detailed discussion of the analytical method is given.

KEYWORDS: Ni-based Superalloy, Creep Rupture, Damage Mechanics, Life Prediction, Constitutive Modeling

1. INTRODUCTION

Nickel-base superalloys are often used in the aerospace, power generation, and pressure vessel and piping industries where operating temperatures and loads necessitate materials with suitable creep resistance. Under some conditions the creep behavior of nickel-base superalloys is dominated by the tertiary creep regime, where primary and secondary regimes are subordinate [1].

Creep deformation is defined in three distinct stages: primary, secondary, and tertiary as depicted in Figure 1. Creep is sensitive to stress and temperature. Diffusion flow, dislocation slip and climb, and grain boundary sliding are all basic mechanisms of creep. Diffusion flow occurs under low stress and high temperature where atomic diffusion and the

applied load lead to elongated grains. Dislocation slip and climb is the fundamental mechanism for primary and secondary creep stages where initially strain hardening occurs until a saturation of dislocation density together with high temperature provides a balancing recovery mechanic. Grain boundary sliding is the fundamental mechanism for tertiary creep where small cavities coalesce into large voids causing a non-linear reduction in creep strength ultimately leading to rupture [2,3].

Early work focused on modeling the minimum creep rate and predicting creep rupture through Norton's power law and either the Larson-Miller Parameter or Monkman-Grant method respectively [4-6]. In all three, the required material constants can be analytical determined from experimental data; however, the Norton power law is not appropriate for the creep behavior of nickel-base superalloys as it does not model the tertiary creep regime [7].

Thus Kachanov [8] and Rabotnov [9] developed constitutive equations which model both secondary and tertiary creep. The Kachanov-Rabotnov equations have been found to accurately model the creep behavior of a number of nickel-base alloys; however, an approach to determine the material constants analytically from experimental data has yet to be developed. Researchers often resort to computationally expensive numerical optimization or dexterous manual iteration to determine appropriate material constants [10]. This issue has severely limited the application of the Kachanov-Rabotnov equations.

A novel method has been developed to analytical determine the Kachanov-Rabotnov material constants from experimental data. Previous research has provided numerical optimized material constants for DS GTD-111 [10]. A comparison between these constants and those developed by the new approach is provided. The difference between the

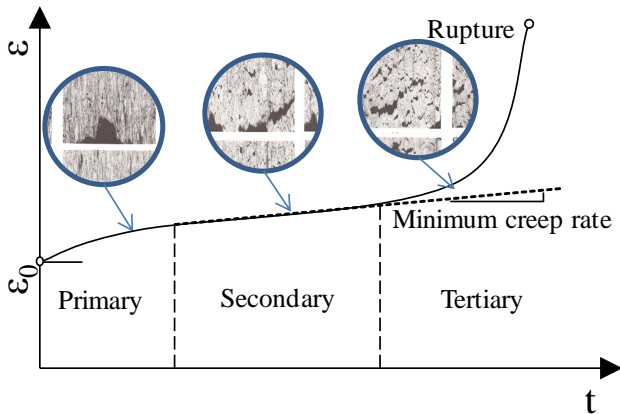


Figure 1 – Creep Deformation

creep deformation, damage evolution, rupture time prediction, and critical damage prediction produced using the two methods is discussed.

2. CONSTITUTIVE MODEL

The classical approach to modeling the secondary creep behavior for materials is the Norton power law for secondary creep [4]

$$\dot{\varepsilon}_{cr} = \frac{d\varepsilon_{cr}}{dt} = A\bar{\sigma}^n \quad (1)$$

where A and n are the secondary creep constants, and $\bar{\sigma}$ is an equivalent stress. The Norton power law is sometimes referred to as the Norton-Bailey law. The secondary creep constants A and n exhibit temperature-dependence. Stress provides a substantial contribution to the creep strain rate as the n secondary creep constant is an exponent of stress. The A and n constants can be determined by setting Norton's power law for secondary creep equal to the minimum creep strain rate. Dorn [11] suggests that temperature contributions can be accounted for by replacing the A constant with an Arrhenius equation

$$A(T) = B \exp\left(\frac{-Q_{cr}}{RT}\right) \quad (2)$$

where B is the pre-exponential factor in units $MPa^{-1} hr^{-1}$, Q_{cr} is the apparent activation energy for creep deformation in units $J mol^{-1}$, R is the universal gas constant $8.314 J mol^{-1} K$, and T is temperature in units Kelvin. Introducing Eq. (1) into Eq. (2) leads to

$$\dot{\varepsilon}_{cr} = \frac{d\varepsilon_{cr}}{dt} = B\bar{\sigma}^n \exp\left(\frac{-Q_{cr}}{RT}\right) \quad (3)$$

Using this equation, stress and temperature contributions to the strain rate are obtained. The secondary creep constants can be determined from uniaxial creep tests by rearranged Eq. (3) into the following form

$$\ln \dot{\varepsilon}_{min} = \ln B + n \ln \bar{\sigma} - \frac{Q_{cr}}{RT} \quad (4)$$

where the creep strain rate $\dot{\varepsilon}_{cr}$ is replaced with the minimum creep strain rate $\dot{\varepsilon}_{min}$. Plotting the log of the minimum creep

strain versus $1/T$, the apparent activation energy of creep, Q_{cr} , can be determined as the slope. Plotting the log of the minimum creep strain versus von Mises equivalent stress, the secondary creep constant, n , is the slope.

Creep damage takes the form of defects such as microcracks, cavities, voids, etc. within a material. The tertiary creep regime is where most creep damage occurs. Microstructurally, grain boundary sliding occurs where small cavities coalesce into large voids causing a non-linear reduction in creep strength ultimately leading to an accelerating creep strain rate and rupture [2]. Under high stress and temperature conditions the tertiary creep regime is dominant; therefore, a damage model is necessary. Kachanov [8] and Rabotnov [9] proposed interfacing the Continuum Damage Mechanics (CDM) framework with the proven Norton power law for secondary creep. In CDM, damage, ω , is assumed to be homogenous and irreversible. The Kachanov-Rabotnov [9] coupled creep-damage constitutive equations are as follows

$$\dot{\varepsilon}_{cr} = \frac{d\varepsilon_{cr}}{dt} = A \left(\frac{\bar{\sigma}}{1-\omega} \right)^n \quad (5)$$

$$\dot{\omega} = \frac{d\omega}{dt} = \frac{M\bar{\sigma}^\chi}{(1-\omega)^\phi} \quad (6)$$

where A and n are the Norton power law constants, $\bar{\sigma}$ is von Mises stress, and M , χ , and ϕ are tertiary creep damage constants. The Norton power law constants A and n can be easily determined using the analytical approach discussed previously. For the tertiary creep damage constants M , χ , and ϕ there is no analytical method; therefore, numerical optimization and/or manual iteration is implemented. There are many forms of the Kachanov-Rabotnov constitutive model found in literature [12,13,14]. It has been used for a number of materials [15].

A useful property of the Kachanov-Rabotnov constitutive equations is rupture can be predicted by integration of the damage evolution equation [Eq. (6)] as follows

$$(1-\omega)^\phi d\omega = M\sigma_r^\chi dt$$

$$-\frac{(1-\omega)^\phi}{1+\phi} \Big|_{\omega_0}^{\omega} = M\sigma_r^\chi \Big|_{t_0}^t \quad (7)$$

under the conditions that stress and temperature be constant. Assuming initial time, t_0 , and initial damage, ω_0 , equal 0.0, simplification leads to rupture time and damage predictions

$$t = \left[1 - (1-\omega)^{\phi+1} \right] \left[(\phi+1)M\sigma_r^\chi \right]^{-1} \quad (8)$$

$$\omega(t) = 1 - \left[1 - (\phi+1)M\sigma_r^\chi t \right]^{\frac{1}{\phi+1}} \quad (9)$$

To predict rupture time, t_r , the critical damage, ω_{cr} , must be known. It is acceptable to assume that critical damage is equal to unity; however, MacLachlan and Knowles [16] suggest that critical damage is a function of the ultimate tensile strength

(UTS) and net/effective stress, $\bar{\sigma}_{net}$. Rupture is reached when the net/effective stress, is equivalent to the UTS and takes the form

$$\bar{\sigma}_{net} = \frac{\bar{\sigma}}{(1-\omega)} \Rightarrow \omega_f = \frac{UTS - \bar{\sigma}}{UTS} \quad (10)$$

In this paper, a ω_{cr} of unity is assumed.

The Kachanov-Rabotnov constitutive model [Eqs. (5) and (6)] was implemented in ANSYS a general-purpose finite element analysis (FEA) software. The equations were written into a FORTRAN subroutine formatted as an ANSYS user-programmable feature (UPF). The Damage variable, ω was defined as an internal state variable and initialized at 0.0. To prevent a singularity critical damage, ω_{cr} was set to 0.90.

Using the ANSYS parametric design language (APDL), an input deck was written which simulates a uniaxial creep experiment. A single 8-noded block element was used. Appropriate loads, temperatures, and displacements are applied to simulate a uniaxial specimen. Simulated creep deformation, $\varepsilon_{cr}(t)$, was recorded to a data file and subsequently compared with experiments.

3. NUMERICAL OPTIMIZATION

Numerical optimization is the most common method used to find the tertiary creep damage constants. The authors previously developed an automated optimization routine, called uSHARP[17], to determine M , χ , and ϕ tertiary creep damage constants. Boundary conditions were matched to those of experiments and simulations were carried out. The simulated creep deformations were then compared with that of experiments. ANSYS simulations were repeated with the tertiary creep damage constants being iterative optimized until the least squares value between simulate and experimental creep deformation was minimized. The least squares objective function was based on creep strain, and is presented as

$$S = \frac{\sum_{i=1}^m (\varepsilon_{FEM,i} - \varepsilon_{EXP,i})^2}{m} \quad (11)$$

where $\varepsilon_{FEM,i}$ and $\varepsilon_{EXP,i}$ are the strain values obtained by FEA simulation and experimental testing, respectively. The parameter m is the total number of data points in a simulation at a single iteration. The number of data points in the FEA and experimental data always differed, thus an automated smoothing routine was developed to unify the time basis of the data.

To optimize the tertiary creep damage constants the simulated annealing multimodal (SAM) algorithm was implemented in the uSHARP routine [18,19]. The SAM algorithm is a global optimizer capable of both uphill and downhill moves; therefore, it is capable of climbing out of local minima.

The uSHARP routine executes ANSYS at each iteration; ANSYS runs the input deck and runs a single simulation; uSHARP evaluates the objective function, then issues the

SAM algorithm and updates the guess for the material constants. This process is repeated until the difference between least square values meets termination criteria.

To reduce solve time, a suitable solve space needed to be resolved. The highest and lowest temperature experiments were optimized first. Using these experiments the target range for tertiary creep damage constants was set as $0.0 \leq M \leq 700$, $1.7 \leq \chi \leq 2.3$, and $0.0 \leq \phi \leq 60$. To produce initial guess constants, the rupture prediction model [Eq. (8)], was compared with experimental data. Manual iteration was performed until the initial guess constants produced a rupture time equal to the experiment.

The Kachanov-Rabotnov constitutive equations do not account for primary creep. Primary creep strain was approximated from experimental data and added to the simulate creep deformation within uSHARP.

4. ANALYTICAL METHOD

A novel analytical method has been developed to determine the tertiary creep damage constants for the Kachanov-Rabotnov constitutive model. Examining the constitutive model, it is observed that while the constants for the creep strain rate equation [Eq. (5)] can be found directly from experimental data (using the minimum creep strain rate as previously mentioned), the constants for the damage evolution equation [Eq. (6)] cannot. The damage evolution equation is a function of damage; therefore, a method is needed to find damage from creep deformation. First the creep strain rate is found from experimental data using differencing

$$\dot{\varepsilon}_{cr}^{i+1} = \frac{\varepsilon_{cr}^{i+1} - \varepsilon_{cr}^i}{\Delta t}, \quad \Delta t = t_{i+1} - t_i \quad (12)$$

Next using algebraic manipulation of the creep strain rate [Eq. (5)], the damage, ω , at each time step can be determined

$$\omega(\dot{\varepsilon}_{cr}) = \frac{\left(\frac{\dot{\varepsilon}_{cr}}{A}\right)^{1/n} - \sigma}{\left(\frac{\dot{\varepsilon}_{cr}}{A}\right)^{1/n}} \quad (13)$$

Depending on the accuracy of the selected A and n constants (determined from the minimum creep strain rate) and quantity and quality of time steps available, the finite differenced damage data may exhibit some non-uniformity. At time zero, the values of damage found will be high. This is attributed to the high creep strain rate observed in the primary creep regime. The Kachanov-Rabotnov constitutive model does not account for the strain hardening of primary creep. To fix this issue, the damage data should be modified such that damage is set to zero until the minimum creep strain rate is reached. With the damage at each time step known, the damage rate can be easily derived using differencing

$$\dot{\omega}_{cr}^{i+1} = \frac{\omega_{cr}^{i+1} - \omega_{cr}^i}{\Delta t}, \quad \Delta t = t_{i+1} - t_i \quad (14)$$

With both the damage and damage rate found, enough information is known to model damage evolution.

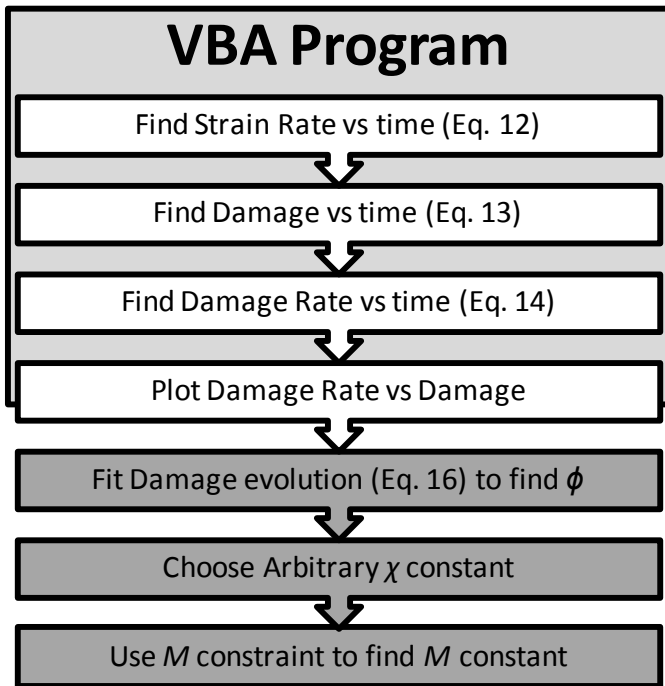


Figure 2 – Analytical Method

Using suitable regression analysis software the damage evolution equation [Eq. (6)] can be written as a user-defined equation and the tertiary creep damage constants be determined.

When the damage evolution equation is parametrically exercised, it is observed that three tertiary creep damage constants far exceeds the number necessary to accurately fit data. This excess number of constants reduces the individual dependency resulting in an ill-defined equation. Further

simplification can be done to reduce the number of independent constants. To that end, the rupture prediction model is algebraic manipulated to find an M constraint as follows

$$M = \frac{1 - (1 - \omega_{cr})^{\phi+1}}{(\phi + 1) \bar{\sigma}^{\chi} t_r} \quad (15)$$

where the critical damage, ω_{cr} is equal to the final value found analytical from the experimental data, and t_r is the rupture time. This M constraint is introduced into the damage evolution equation [Eq. (6)] furnishing

$$\dot{\omega}(\omega) = \frac{1 - (1 - \omega_{cr})^{\phi+1}}{(\phi + 1) \bar{\sigma}^{\chi} t_r} \bar{\sigma}^{\chi} = \frac{1 - (1 - \omega_{cr})^{\phi+1}}{(1 - \omega)^{\phi} (\phi + 1) t_r} \quad (16)$$

where equivalent stress, $\bar{\sigma}$, and both the M and χ tertiary creep damage constants are eliminated. Comparing the updated damage evolution equation to that of Kachanov-Rabotnov, it is determined that the constants M and χ are dependent while ϕ is independent. When using the Kachanov-Rabotnov approach, the constant χ should be chosen arbitrarily. The constant M should be found using the constraint equation [Eq. (15)]. These steps produce a well-defined equation designed to satisfy experimental conditions.

Difficulty arises when dealing with a set of experiments conducted at different stress levels with a set temperature. Using the Kachanov-Rabotnov damage evolution equation [Eq. (6)] without the new constraint, the problem expands to a 3D problem $\dot{\omega}(\sigma, \omega)$ where stress influence damage behavior. When considering the new constraints within the damage evolution model, [Eq. (16)], the problem expands to a 4D problem $\dot{\omega}(\omega, \omega_{cr}, t_r)$ where critical damage and rupture

Table 1 – Creep deformation and rupture data for DS GTD-111 [20]

	Orientation	Primary Strain, ε_{pr}	Temperature, T (C)	Stress, σ (MPa)	Rupture Time, t_r (hr)	Critical Damage, ω_{cr}	Rupture Strain, ε_r
1	L	1.27E-03	649	896	466	0.161	0.049
2	L	3.04E-03	760	408	5624	0.314	0.150
3	L	2.44E-03	760	613	244	0.324	0.132
4	T	6.00E-03	760	517	376	0.436	0.069
5	T	3.60E-03	760	613	43	0.217	0.018
6	L	2.60E-03	816	455	322	0.445	0.215
7	T	2.12E-03	816	455	127	0.292	0.046
8	L	NA	871	241	2149	0.603	0.188
9	L	8.50E-04	871	289	672	0.461	0.117
10	T	1.92E-04	871	241	980	0.601	0.076
11	T	2.03E-03	871	289	635	0.242	0.051
12	L	6.55E-04	940	244	69	0.352	0.141
13	T	7.07E-04	940	244	63	0.454	0.038
14	L	1.32E-04	982	124	821	0.571	0.178
15	L	NA	982	145	302	0.507	0.091
16	45°	5.00E-03	871	289	455	0.358	0.060

Table 2 - Secondary creep constants of the Norton power law for DS GTD-111 [7]

Temperature (°C)	<i>n</i>		<i>A</i>	
	L	T	L	T
649	8.500		5.909E-30	
760	7.591	10.890	1.393E-25	8.090E-35
816	7.000	9.650	2.477E-23	3.572E-30
871	6.507	6.516	5.764E-21	3.480E-21
940	6.000	4.850	3.507E-18	4.210E-16
982	5.547		8.290E-17	

time influence damage behavior. In all cases, advanced regression analysis software is required. Temperature-dependence of the constants must be introduced post regression fitting, using any suitable equation which matches the experimental trend. Ideally, the Arrhenius Eq. (2), would be used. In this paper, the 3D and 4D problem is left for later study. In this study, the constants experiments at the same temperature with different stress levels are determined independently.

To implement the analytical method a Microsoft Excel program was written using the visual basic for applications (VBA) programming language. The stress, temperature, rupture time, estimated primary creep strain, and secondary creep constants *A* and *n* as well as a text file of the creep deformation are input. The program then automatically produces damage and damage rate data using the previously outlined method. Using suitable regression analysis software the tertiary creep damage constants are determined. An illustration of this process is provided in Figure 2.

5. RESULTS & DISCUSSION

The subject material chosen is DS GTD-111, a directionally solidified dual-phase γ - γ' Ni-based superalloy. The material is transversely-isotropic with a columnar grain in the longitudinal (L) direction and isotropy found on the transverse (T) plane. Creep deformation experiments were conducted on L and T-oriented specimen of DS GTD-111 according to an ASTM standard E-139 [21] for a range of temperature and stress conditions. A list of the experiments conducted with properties is provided in Table 1.

Taking the creep deformation data from experiments, differencing was used to determine the creep strain rate. From this data, the minimum creep strain rate was found for each experiment and secondary creep constants determined. The secondary creep constants are listed in Table 2.

5.1. Numerical Optimization

A number of issues arose when implementing numerical optimization for DS GTD-111. Long solve times were a major problem. The average number of iterations to convergence was 8390 with a minimum and maximum value of 1539 and 18585, respectively. To reduce solve-time, the maximum time-step size allowable was increased to a factor of $t_r/10$ or greater. This resulted in solve-time per iteration varying between 15-60 seconds. Generally, the simulated annealing routine performed well but in some cases it was unable to find suitable constants. In these experiments, strain softening beyond the minimum creep rate was minimal. As a consequence, the creep damage parameters could not properly be optimized by uSHARP. Instead, the values for the material constants were obtained manually until a suitable set of constants could be realized.

Table 3 – Optimized [10] and Analytically determine tertiary creep damage constants for DS GTD-111

	Temperature, <i>T</i> (C)	Stress, σ (MPa)	Optimized			FOM		Analytical			FOM
			<i>M</i> ($MPa^{\chi}hr^{-1}$)	χ	ϕ	(%)	<i>M</i> ($MPa^{\chi}hr^{-1}$)	χ	ϕ	(%)	
L	649	896	10.000	1.880	55.000	32.5	0.010	3.000	27.250	0.5	
L	760	408	20.847	1.900	8.500	4.8	0.026	3.000	8.641	3.8	
L	760	613	19.784	2.231	13.261	26.8	0.171	3.000	9.210	3.7	
T	760	517	36.161	2.106	14.810	26.9	0.183	3.000	9.500	1.3	
T	760	613	51.801	2.203	39.931	34.6	0.453	3.000	21.400	1.2	
L	816	455	64.127	2.257	3.792	10.9	0.647	3.000	3.800	4.6	
T	816	455	167.590	1.981	28.224	30.1	0.550	3.000	14.110	1.0	
L	871	241	96.015	2.022	7.161	25.0	0.474	3.000	6.000	1.0	
L	871	289	131.010	2.054	9.698	19.4	0.682	3.000	8.000	1.9	
T	871	241	263.010	2.098	2.296	17.2	1.210	3.000	5.000	0.6	
T	871	289	345.840	1.919	6.823	6.9	0.754	3.000	6.628	5.4	
L	940	244	579.120	2.310	7.069	6.0	15.267	3.000	5.100	2.7	
T	940	244	600.000	2.290	7.069	20.5	10.709	3.000	9.261	2.5	
L	982	124	655.930	2.221	3.278	4.5	14.529	3.000	3.278	2.4	
L	982	145	665.200	2.288	5.126	17.1	19.496	3.000	4.467	3.5	
45°	871	289	53.296	2.156	20.933	28.6	0.623	3.000	13.590	0.7	

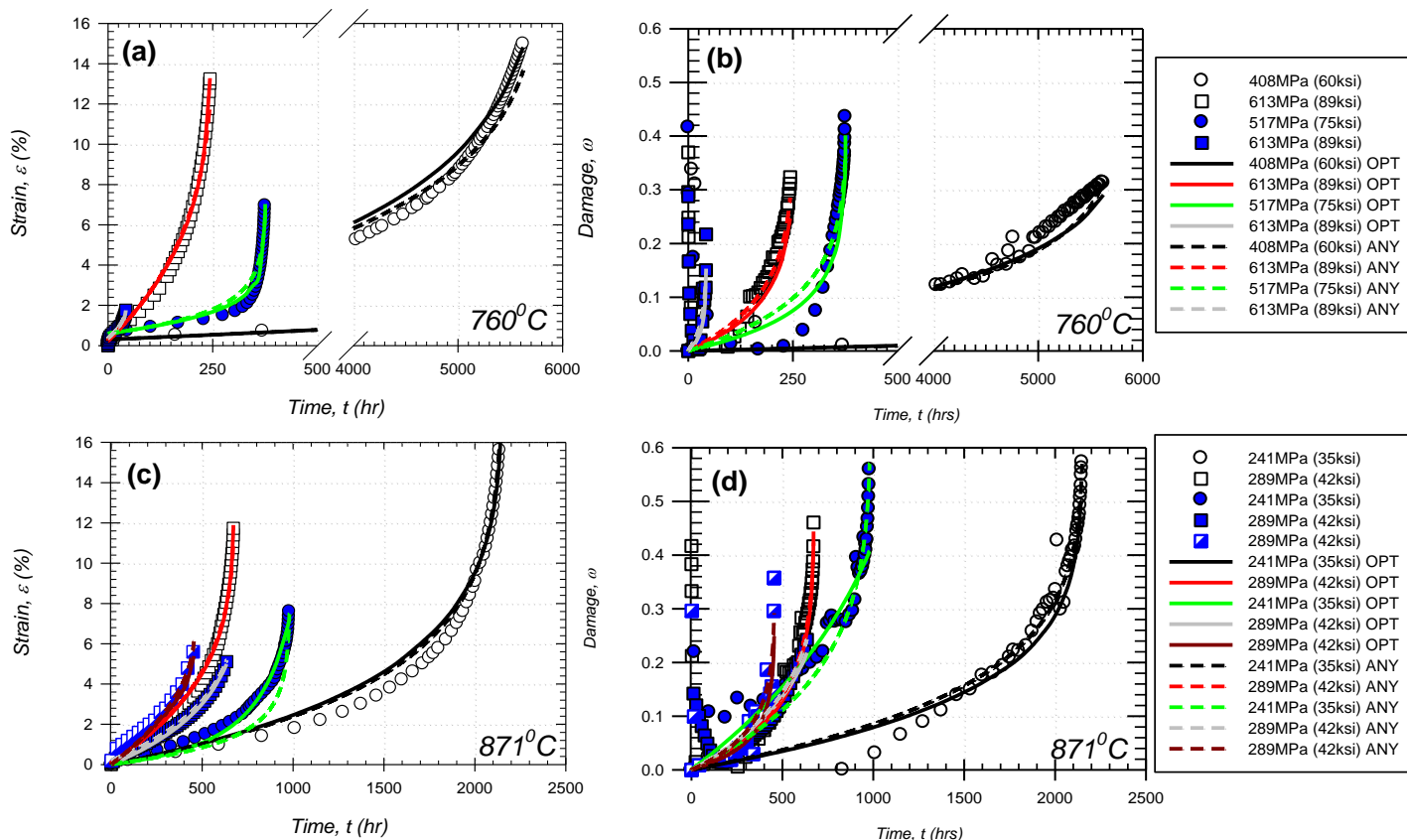


Figure 3 - Creep deformation and damage evolution fits of L (open) and T (filled) DS GTD-111 at 760 and 871°C

5.2. Analytical Method

A number of issues arose when implementing the analytical method for DS GTD-111. The creep deformation data in some cases, was not recorded with enough significant figures such that different strains were recorded repeatedly for the same hour. This resulted in Not a Number (NaN) values of creep strain rate, damage, and damage rate. To alleviate this problem the data had to be manually cleaned. The regression software produced the best fit for damage evolution but that did not always result in a best fit for creep deformation. In tests 4, 7, and 10 a significant portion of life was spent in the secondary creep regime. It was difficult to fit the constitutive model to these data because the damage evolution equation [Eq. (6)] does not include a time-hardening term. For most experiments, limited manual adjustment of the damage evolution curve was conducted to develop slightly improved creep deformation results.

5.3. Discussion

Both numerical optimization and the analytical method were implemented and tertiary creep damage constants were found as listed in Table 3. A figure of merit (FOM) was developed to judge the goodness of fit of the constants. The FOM is the average percent error of absolute rupture time

prediction, rupture strain FEM, and critical damage prediction compared to experimental data and is as follows

$$FOM = \left| \frac{t_{r,PRED} - t_r}{t_r} \cdot 100 \right| + \left| \frac{\varepsilon_{r,FEM} - \varepsilon_r}{\varepsilon_r} \cdot 100 \right| + \left| \frac{\omega_{cr,PRED} - \omega_{cr}}{\omega_{cr}} \cdot 100 \right| \quad (17)$$

The FOM results can be found in Table 3. The analytical method produced much lower FOMs compared to numerical optimization. This is attributed to the highly inaccurate predicts of critical damage the numerical optimized constants produced. The analytical method directly includes experimental critical damage in the M constraint; therefore it always produced an accurate critical damage prediction. Using numerical optimization the average error of the rupture time prediction, rupture strain FEM, and critical damage was 9.08%, 5.09%, and 44.88% respectively. Using the analytical method the average errors are 2.50%, 2.32%, and 0.11% respectively. This clearly shows that the analytical method produces a more accurate set of constants.

Creep deformation and damage evolution curves for DS GTD-111 at 760 and 871°C are provided in Figure 3. The numerical optimized curves (OPT) are solid lines and the analytical method (ANY) curves are dotted lines.

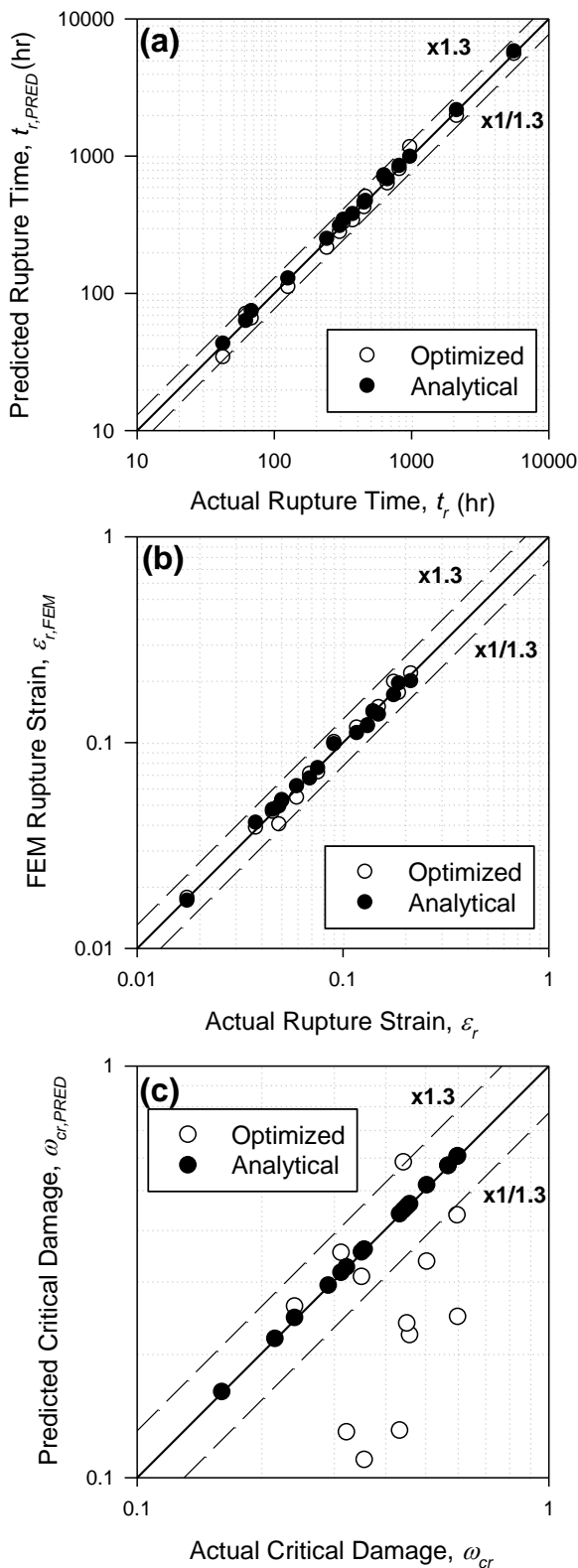


Figure 4 - Predictions of (a) creep rupture, (b), rupture strain and (c) critical damage

It is observed that in most cases the difference between the results achieved with both models is negligible. The experiments at 517MPa 760°C and 241MPa 871°C show that the analytical method does not always produce a best fit to creep deformation. The 241MPa 871°C experiment demonstrates that a better damage evolution fit does not always produce a better creep deformation fit. Overall, these curves demonstrate that the analytical approach can produce highly accurate fits to creep deformation data from experiments using a more straightforward approach compared to numerical optimization.

A depiction of rupture time prediction, rupture strain FEM, and critical damage prediction compared to experimental data is provided in Figure 4. It is observed that in terms of rupture time predictions and rupture strain FEM both numerical optimization and the analytical method performed well. The numerical optimized critical damage predicts do not follow the experimental results.

Because larger time-steps were used during optimization, when reducing the maximum time-step size using the numerical optimized constants, the creep deformation can diverge. This is due to the fact that the constants are numerically optimized to a discrete time-step. The advantage of the analytical method is that the constants are not dependent on time-step size. The constants are a product of fitting damage evolution analytically and therefore are always numerically stable. Decreasing the time-step when using the analytical constants increases the accuracy of the creep deformation fits. In this study, the maximum time-step size used for the analytical method was 1hr.

6. CONCLUSION

The analytical method has been found to produce better creep deformation fits, rupture time predictions, rupture strain FEM, and critical damage predictions when compared to numerical optimization. Introducing the M constraint to the Kachanov-Rabotnov damage evolution equation has resulted in a more well-defined equation founded on experimental conditions. The analytical method proves to be a way that tertiary creep damage constants can be quickly determined without the need for extensive numerically or manually iterative processes. Numerically stable constants can be determined analytically and rapidly. Future work will focus on dealing with the difficulty that arises when dealing with a set of experiments conducted at different stress levels with a set temperature.

7. ACKNOWLEDGEMENTS

Calvin Stewart is thankful for the support of a McKnight Doctoral Fellowship through the Florida Education Fund. Ali P. Gordon recognizes the support of the Florida Center for Advanced Aero-Propulsion (FCAAP).

REFERENCES

- [1] National Research Council (U.S.) Committee on Materials for Large Land-Based Gas Turbines, 1986, "Materials for large land-based gas turbines," National Academy Press.
- [2] Penny, R. K., and Marriott, D. L., 1995, *Design for Creep*, Springer, New York, NY.
- [3] Stewart, C. M., and Gordon, A. P., 2010, "Modeling the Tertiary Creep Damage Behavior of a Transversely-Isotropic Material under Multiaxial and Periodic Loading Conditions," ASME 2010 Pressure Vessel and Piping Conference, PVP2010-25041, Bellevue, WA, July 18-22.
- [4] Norton, F. H., 1929, *The creep of steel at high temperatures*, McGraw-Hill, London.
- [5] Larson, R. and Miller, J., 1952, *Trans. ASME*, **74**, pp. 765.
- [6] Monkman, F. and Grant, N., 1956, *Proc. ASTM*, **56**, p. 595.
- [7] Stewart, C. M., and Gordon, A. P., 2010, "A Creep Rupture Time Model for Anisotropic Creep-Damage of Transversely-Isotropic Materials," ASME TURBOEXPO 2010, GT2010-22532, Glasgow, UK, June 14-18, 2010.
- [8] Kachanov, L. M., 1967, *The Theory of Creep*, National Lending Library for Science and Technology, Boston Spa, England, Chaps. IX, X.
- [9] Rabotnov, Y. N., 1969, *Creep Problems in Structural Members*, North Holland, Amsterdam.
- [10] Stewart, C. M., Hogan, E. A., and Gordon, A. P., 2009, "Modeling the Temperature-Dependence of Tertiary Creep Damage of a Directionally Solidified Ni-Base Superalloy," ASME IMECE 2009, IMECE2009-11288, Lake Buena Vista, Florida, November 13-19, 2009.
- [11] Dorn, J.E., 1955, "Some Fundamental experiments on high temperature creep", *Journal of the Mechanics and Physics of Solids*, **3**, pp. 85-116.
- [12] Stewart, C. M., Gordon, A. P., and Nicholson, D. W., 2009, "Numerical Simulation of Temperature-Dependent, Anisotropic Tertiary Creep Damage," *47th AIAA Aerospace Sciences Meeting Including The New Horizons Forum and Aerospace Exposition*, Orlando, FL, Jan. 5-8th.
- [13] Stewart, C. M., and Gordon, A. P., 2009, "A Novel Anisotropic Tertiary Creep Damage Model for Transversely Isotropic Materials," *Proceedings of the 12th International Conference on Pressure Vessel Technology*, Jeju Island, KOREA, Sept. 20-23rd.
- [14] Stewart, C. M., 2009, "Tertiary Creep Damage Modeling of a Transversely Isotropic Ni-Based Superalloy" Master's Thesis, University of Central Florida, Orlando, FL.
- [15] Stewart, C. M., and Gordon, A. P., (2009), "Modeling the Temperature Dependence of Tertiary Creep Damage of a Ni-base Alloy," *Journal of Pressure Vessel Technology*, **131**(5), pp.1-11.
- [16] Maclachlan, D. W. and Knowles, D. M., 2000, "Creep-Behavior Modeling of the Single-Crystal Superalloy CMSX-4," *Metallurgical and Materials Transactions A*, **31**(5), pp. 1401-1411.
- [17] Hogan, E. A., 2009, "An efficient method for the optimization of Viscoplastic constitutive model constants," Honors in the Major Undergraduate Thesis, University of Central Florida, Orlando, FL.
- [18] Corana, A., Marchesi, M., Martini, C., and Ridella, S., 1987, "Minimizing Multimodal Functions of Continuous Variables with the 'Simulated Annealing' Algorithm," *ACM Transactions on Mathematical Software*, **13**(3), pp. 262-280.
- [19] Goffe, W. L., Gary, D. F., and Rogers, J., 1993, "Global Optimization of Statistical Functions with Simulated Annealing," *Journal of Econometrics*, **60**(1/2), pp. 65-100.
- [20] Ibanez, A. R., Srinivasan, V. S., and Saxena, A., 2006, "Creep Deformation and Rupture Behaviour of Directionally-solidified GTD 111 Superalloy," *Fatigue & Fracture of Engineering Materials & Structures*, **29**(12), pp. 1010 – 1020.
- [21] ASTM E-139, "Standard Test Methods for Conducting Creep, Creep-Rupture, and Stress-Rupture Tests of Metallic Materials," No. 03.01, West Conshohocken, PA.